

# A Novel Color Filter Array and Demosaicking Algorithm for Hexagonal Grids

Alexander Fröhlich and Andreas Unterweger  
Salzburg University of Applied Sciences  
Urstein Süd 1  
5412 Puch/Salzburg, Austria

## ABSTRACT

We propose a new color filter array for hexagonal sampling grids and a corresponding demosaicking algorithm. By exploiting properties of the human visual system in their design, we show that our proposed color filter array and its demosaicking algorithm are able to outperform the widely used Bayer pattern with state-of-the-art demosaicking algorithms in terms of both, objective and subjective image quality.

**Keywords:** Hexagonal Sampling, Color Filter Array, Demosaicking

## 1. INTRODUCTION

In most digital cameras a single charge-coupled device (CCD) or complementary metal-oxide-semiconductor (CMOS) sensor array captures the incoming light to form a digital representation of the scene in front of the camera's lens. Such sensors are sensitive to a wide range of light and can therefore only capture monochromatic images. Several techniques have been used to overcome this limitation and to capture color images. The most common one is the use of color filter arrays (CFAs). Each element in the sensor array is equipped with a color filter which lets only pass one of the three primaries red, green or blue. The pattern in which the filters are arranged strongly influences subsequent image processing tasks and the image quality. The most common CFA is the Bayer pattern [1]. It uses twice as much green pixels as red and blue ones exploiting the fact that the human visual system (HVS) is more sensitive to green as compared to red and blue.

Other CFAs exist beside the Bayer pattern. However, all of them are based on a square sampling grid (even though the grid might be rotated  $45^\circ$ ). Square sampling allows for a simple adaption of 1-D signal processing tasks to 2-D signals and is the quasi standard in digital imaging. Although rarely discussed, other sampling lattices are possible. Among them is the hexagonal lattice which offers some promising benefits. Firstly, Mersereau [2] showed that hexagonal sampling requires 13.4% less sampling points than square sampling to store the same information when the input signal is circularly band limited. Secondly, hexagonal sampling provides uniform connectivity and equidistant neighborhood which is advantageous for image processing applications [3]. Finally, hexagonal sampling imitates the human eye more closely as the cones and rods on the retina are roughly placed on a hexagonal grid [4].

A proposal for a CFA for hexagonal grids can be found in [5, 6, 7]. This CFA provides the same number of red, green and blue pixels. Although the high symmetry can be seen as an advantage, it does not consider the properties of the HVS. In contrast, our proposed CFA has a higher ratio of green pixels for increased detail preservation.

In order to create full color images from the data captured with the proposed CFA, a special demosaicking algorithm is used. Many demosaicking algorithms for the Bayer pattern have been introduced in the past. An overview and comparison of algorithms is provided in [8]. Adaptive homogeneity-directed demosaicking [9] is rated among the best of all tested algorithms and thus used in this paper for comparison. The proposed algorithm makes use of several methods described in [8].

This paper is structured as follows: In section 2, we present our hexagonal CFA and its properties as well as a demosaicking algorithm. Subsequently, in section 3, we assess its impact on image quality by comparing it to the commonly used Bayer Pattern before concluding the paper.

We contribute a novel CFA and a corresponding demosaicking algorithm for hexagonal sampling grids and show its superiority in terms of image quality.

## 2. HEXAGONAL DEMOSAICKING

In contrast to the Bayer pattern, color filter arrays for hexagonal grids are usually displayed with equal distribution of red green and blue pixels [5, 6, 7]. The disadvantage of such an assembly is that none of the three channels is able to capture spatial frequencies near the grid's Nyquist frequency. The Bayer pattern contains twice as much green pixels as red or blue ones, so the green channel has a higher spatial resolution [1]. Because of the high correlation between the three color channels in natural images, the high frequency information of the green channel can be used for the reconstruction of the red and blue channels.

We propose a CFA for hexagonal grids which exploits the interchannel correlation similar to the Bayer pattern. Our array is displayed in figure 1. It has a distribution of red, green and blue pixels of 22%, 67% and 11%, respectively. Compared to the Bayer pattern's distribution of 25%, 50% and 25%, the rate of green pixels is higher, while the amount of red and blue pixels is lower. The higher amount of green pixels aims at increasing the frequency which the sensor array is able to capture and reducing subsequent interpolation errors.

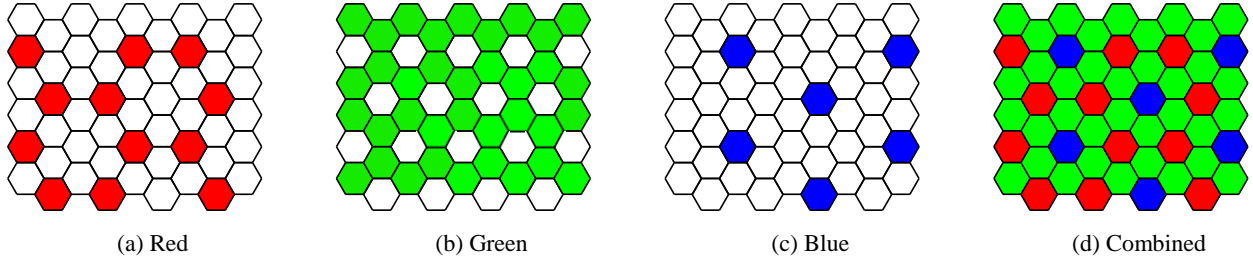


Figure 1. The proposed hexagonal color filter array

To reconstruct a full color image from the data captured with the described CFA, a dedicated demosaicking algorithm has to be used. While other algorithms may be possible, we propose one that uses directional interpolation and exploits interchannel correlation. The steps of the demosaicking process can be summarized as follows: First, three candidate images are created using directional interpolation of the green channel and nondirectional interpolation of red and blue channels. Second, these candidate images are merged to one output image. Third, alias canceling is applied.

Similar to Hirakawa and Park's Adaptive Homogeneity-Directed Demosaicking algorithm [9], we create candidate images for each interpolation direction and decide at each pixel position which one of them to use. As opposed to square grids, hexagonal grids have three axes which have to be considered for directional interpolation. Therefore, three candidate images have to be computed.

The first step in the demosaicking process is to reconstruct the green channel. In the proposed CFA, every non-green (red or blue) pixel is surrounded by two green pixels in each of the six cardinal directions (compare figure 1b). For the directional interpolation of a green value at a red or blue pixel position a 5-tap FIR filter is applied. The filter coefficients can be written as a vector  $h$ . The third coefficient of the vector, representing the pixel in question whose value is unknown, is set to zero.

$$h = [w_{-2} \ w_{-1} \ 0 \ w_{+1} \ w_{+2}] \quad (1)$$

$$w = \begin{cases} 1 & \text{for } x = 0 \\ \text{sinc}(\pi x) \times \text{sinc}\left(\pi \frac{x}{2}\right) & \text{for } -2 < x < 2 \\ 0 & \text{else} \end{cases} \quad (2)$$

A modified Lanczos interpolation kernel is used to compute the filter coefficients. The Lanczos interpolation function is displayed in equation 2 where  $\text{sinc}(x) = \frac{\sin(x)}{x}$ . It has zeros at every integer value of  $x$ . In order to be usable for the interpolation of a missing value between four known values on a given grid,  $x$  must not be defined as the distance between two pixels  $d$ . With  $x=0.65d$ , the minimum of the function matches exactly the position  $2d$ . The resulting filter coefficients are

$$w_{-1} = w_1 = 0.6554, w_{-2} = w_2 = -0.1554 \quad (3)$$

Three candidate images have to be created, each with the green channel interpolated along one cardinal axis. After the green channels have been restored, the red and blue channels need to be restored in each candidate image. First, the red values at blue pixel locations are calculated. Each blue pixel is surrounded by six ( $N=6$ ) red pixels at a distance of  $1.73d$  with  $d$  being the diameter of a pixel from side to side. Based on the assumption that the color channels are highly correlated and their difference is varying slowly, we interpolate the pixel difference  $R-G$  instead of the pixel value  $R$  [8]. This way, high frequency information from the green channel can be used in the red channel. In order to avoid interpolation across edges of objects, the six coefficients for each of the surrounding pixels are weighted using the differences  $G_0-G_n$ , where  $G_0$  is the green value at the location in question and  $G_n$  are the green values of one of the six pixels which are used for interpolation. The missing red value can then be computed as shown in equation 4. The addend  $s$  avoids division by 0 in case  $G_0$  and  $G_n$  are identical. Its value should be chosen small against signal range, e.g., 1% of the highest possible signal value.

$$R_0 = \frac{\sum_{n=1}^N \frac{R_n - G_n}{|G_0 - G_n| + s}}{\sum_{n=1}^N \frac{1}{|G_0 - G_n| + s}} \quad (4)$$

The next step is to compute the blue values at red pixel positions. Each red pixel is surrounded by three ( $N=3$ ) blue pixels at a distance of  $1.73d$ , each of which enclose an angle of  $120^\circ$ . The interpolation procedure is the same as in equation 4 with  $N=3$ . Finally, red and blue values need to be computed for all green pixel positions. Each green pixel is surrounded by three pixels ( $N=3$ ) with distance  $d$  for which the full color information is available. These pixels are used to calculate the missing red and blue values using equation 4. Note that even though the algorithm for the interpolation of red and blue values is the same for each of the three candidate images, the values will differ, because the calculation is based on the green values.

After the three candidate images are created, a decision has to be made at each pixel location from which candidate to take the values. Therefore, a local difference value is computed as the maximum of the sums of squares of differences in each color channel between neighboring pixels' values. Only neighbors in the direction of the interpolation of the candidate image are used, e.g., the pixels above and below the pixel in question in the vertically interpolated candidate image. Similar to the homogeneity measure in [9], this measure is performed in CIE-LAB color space to improve accuracy. The computed local difference value is stored in a map. Finally, at each pixel location, the lowest of the three local difference values is used to determine from which candidate image to take the RGB values for the output image. In order to avoid repetitive changes in the interpolation direction between consecutive pixels which would lead to visible artifacts, the map of local differences is filtered before creating the output image. For this, a 2-D FIR filter where the center value is  $1/2$  and the six surrounding values are  $1/12$  is used. Note that the filtering is performed on the hexagonal grid and the filter kernel has a hexagonal shape.

Alias canceling has to be applied after demosaicking to reduce color artifacts. Alias canceling uses a median filter to remove distortions in  $R-G$  and  $B-G$  as displayed in equation 5.  $median_{hex}()$  is a median filter for hexagonal grids with a span of three pixels in each direction, thus covering an area of seven pixels. As opposed to Hirakawa's method [9], alias canceling is not applied to the green channel. Repeated application of the described alias canceling is possible. Best results were achieved with two iterations.

$$R' = G + median_{hex}(R - G), B' = G + median_{hex}(B - G) \quad (5)$$

### 3. EVALUATION

In order to evaluate the effectiveness of the proposed CFA and demosaicking algorithm, it was tested against the Kodak image set (downloaded from [http://www.math.purdue.edu/~lucier/PHOTO\\_CD/](http://www.math.purdue.edu/~lucier/PHOTO_CD/)). The results were compared to those of the same images processed with the algorithm described in [9]. We used the images at the highest available resolution ( $3072 * 2048$ ) and resampled them to  $826 * 477$  using a hexagonal grid and  $768 * 512$  using a square grid, respectively. The pixel counts are slightly different due to misalignment of the hexagonal grid and the original image at the borders. Before resampling, the original images were filtered using a simulated birefringent anti-alias filter. Such filters are used in digital cameras to avoid aliasing, which is caused by signals exceeding the sensor's (CFA's) Nyquist frequency [10]. After resampling, color filter patterns were applied to the square and hexagonally sampled images and the images were demosaicked. For displaying and visual inspection the hexagonally sampled images were then converted into a rectangular grid with  $826 * 954$  pixels and into a square grid with  $826 * 550$  pixels. While the first preserves all details but has an incorrect aspect ratio, the latter provides a corrected aspect ratio but may suffer from loss of detail due to the resizing. All described tasks (filtering, resampling and demosaicking) have been implemented in Matlab.

| Image  | Red            |                | Green          |                | Blue           |                |
|--------|----------------|----------------|----------------|----------------|----------------|----------------|
|        | Bayer          | proposed       | Bayer          | proposed       | Bayer          | proposed       |
| 1      | 42,4157        | <b>42,6012</b> | <b>49,5523</b> | 47,1316        | <b>46,2564</b> | 43,7951        |
| 2      | 36,2505        | <b>37,2600</b> | 45,5201        | <b>48,6111</b> | <b>42,9541</b> | 42,7069        |
| 3      | 45,2612        | <b>46,9760</b> | 51,7253        | <b>56,8393</b> | <b>46,5041</b> | 46,0203        |
| 4      | 37,7535        | <b>38,9507</b> | 45,4686        | <b>49,3832</b> | <b>44,5703</b> | 43,8619        |
| 5      | 39,2035        | <b>40,2725</b> | 44,9679        | <b>47,7153</b> | <b>39,8230</b> | 39,7255        |
| 6      | <b>44,2478</b> | 44,1898        | <b>50,9724</b> | 50,1446        | <b>46,7047</b> | 45,8030        |
| 7      | 44,0371        | <b>45,3688</b> | 49,1533        | <b>54,8329</b> | <b>42,6966</b> | 42,6636        |
| 8      | 40,7823        | <b>40,8741</b> | <b>46,7923</b> | 46,4663        | <b>41,5582</b> | 40,9019        |
| 9      | 46,6925        | <b>47,1335</b> | 52,8848        | <b>54,5782</b> | <b>46,1271</b> | 45,6028        |
| 10     | 45,6162        | <b>46,0573</b> | 51,8773        | <b>54,1592</b> | <b>47,3357</b> | 46,8954        |
| 11     | 41,2007        | <b>41,7460</b> | 48,9978        | <b>50,2105</b> | <b>45,3952</b> | 45,1735        |
| 12     | 47,1038        | <b>48,4788</b> | 54,2571        | <b>56,1061</b> | <b>49,0608</b> | 47,9308        |
| 13     | <b>41,8374</b> | 41,1236        | <b>44,7709</b> | 43,9969        | <b>39,7241</b> | 38,6006        |
| 14     | 36,9653        | <b>38,6590</b> | 45,1788        | <b>49,4877</b> | 39,8797        | <b>40,2035</b> |
| 15     | 39,3446        | <b>40,0926</b> | 47,8342        | <b>52,7363</b> | <b>45,2902</b> | 45,2869        |
| 16     | <b>48,5955</b> | 47,9614        | <b>53,9720</b> | 52,5775        | <b>47,5408</b> | 46,7088        |
| 17     | 47,5142        | <b>48,0096</b> | 51,6417        | <b>52,9261</b> | <b>45,9006</b> | 44,8686        |
| 18     | 39,7277        | <b>40,1537</b> | 45,2550        | <b>46,5020</b> | <b>40,0126</b> | 39,2446        |
| 19     | 45,1325        | <b>45,3379</b> | 50,0165        | <b>50,7916</b> | <b>44,7112</b> | 43,9246        |
| 20     | 46,6980        | <b>46,7141</b> | 51,2243        | <b>52,2659</b> | <b>45,4787</b> | 45,0867        |
| 21     | 45,1846        | <b>45,3648</b> | <b>49,6124</b> | 48,7926        | <b>44,6599</b> | 43,4793        |
| 22     | 42,1740        | <b>42,6437</b> | 46,7815        | <b>50,4672</b> | <b>41,7681</b> | 40,8755        |
| 23     | 43,5124        | <b>44,8317</b> | 50,7412        | <b>55,3703</b> | <b>46,0230</b> | 45,1676        |
| 24     | 42,4831        | <b>42,6646</b> | <b>47,6060</b> | 47,0306        | <b>42,9989</b> | 41,5287        |
| mean   | 42,9056        | <b>43,4777</b> | 49,0335        | <b>50,7968</b> | <b>44,2906</b> | 43,5857        |
| median | 42,9978        | <b>43,4272</b> | 49,3528        | <b>50,3388</b> | <b>45,0007</b> | 43,8932        |

Table 1. PSNR values for images of the Kodak image set processed with the Bayer pattern and Hirakawa and Park's algorithm [9] and the proposed CFA and demosaicking algorithm

To determine the quality of the demosaicking process, the PSNR of each color channel of the demosaicked images was measured with the images without a color filter array applied as reference. Table 1 displays the results of this measure. The proposed CFA and demosaicking algorithm has better PSNR values for red and green channels in a majority of test images. Due to the small number of blue pixels, PSNR values of the blue channel are slightly lower than with the Bayer pattern.

As objective quality measures like PSNR do not always represent the perceived visual quality of an image, the images were also analyzed visually. Figure 2 shows details of the processed images, highlighting the differences between the traditional Bayer pattern and the proposed algorithm. From these samples it can be clearly seen that even though the input images have been filtered with a birefringent anti-alias filter, the Bayer images show strong artifacts. Checkerboard patterns are visible at the edges of objects (e.g., in figure 2c, bottom) and diagonal lines (e.g., in figure 2i, bottom). While errors can also be found in the hexagonally processed images (e.g., occasional color smearing like in 2l, bottom), those are less pronounced than the Bayer pattern's errors. The test images also show advantages of the hexagonal sampling concerning resolution. Even though the hexagonally sampled images tend to appear soft, they retain detail which is lost in square sampled images. E.g., in figure 2g the pixel structure is clearly visible on the window sill, while in figure 2h the window sill can be easily recognized without a distracting grid being visible. The complete set of processed images can be downloaded from <http://goo.gl/le86w0>.

#### 4. CONCLUSION

We proposed a new color filter array for hexagonal sampling grids and a corresponding demosaicking algorithm. By comparing it to the Bayer pattern with Hirakawa's demosaicking approach, we showed that the red and green channels can be reconstructed with higher visual fidelity using our method, while obtaining slightly degraded performance for the blue channel. Furthermore, we showed that our proposed color filter array and demosaicking algorithm significantly reduce artifacts like checkerboard patterns and steps at diagonal edges.

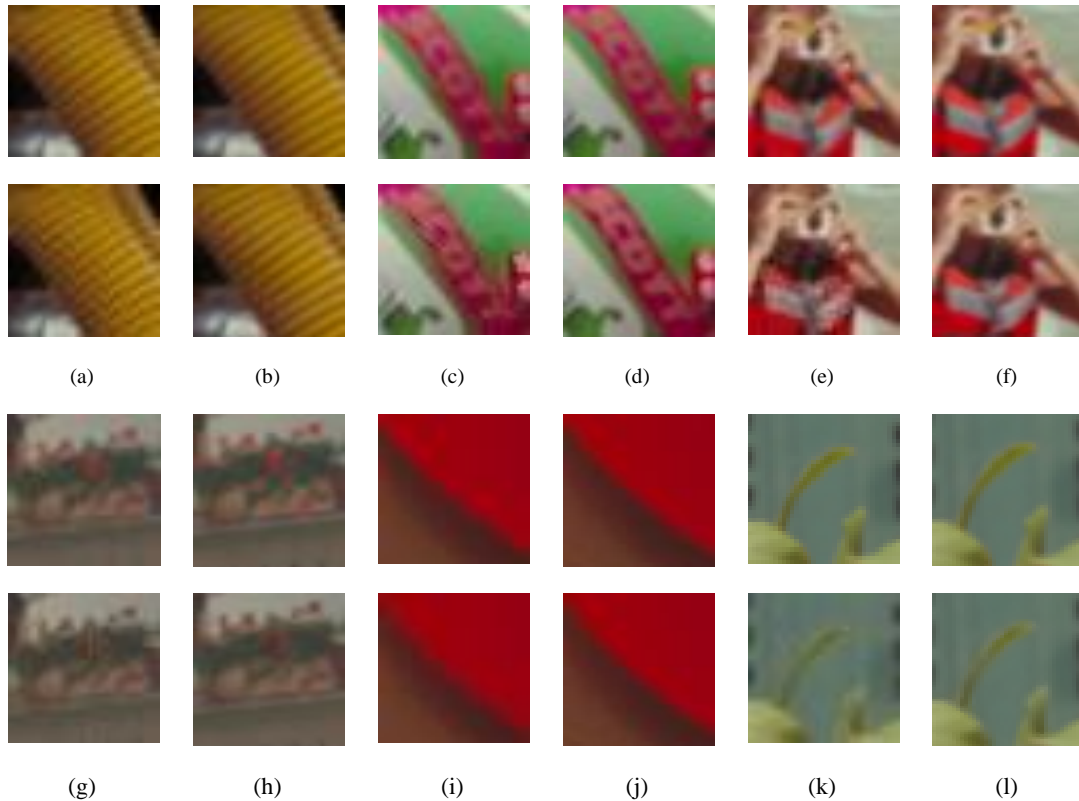


Figure 2. Details of images from the Kodak image set processed using the Bayer pattern and the algorithm from [9] (a, c, e, g, i, k, bottom) and the proposed pattern and algorithm (b, d, f, h, l, bottom). The top rows display unprocessed square-sampled and hexagonally sampled images for reference. Hexagonal images have been transformed to rectangular (non-square) grids and therefore show higher pixel count than square-sampled images.

## REFERENCES

- [1] B. E. Bayer, "Color imaging array," United States Patent 3,971,065, 1976.
- [2] R. M. Mersereau, "The processing of hexagonally sampled two-dimensional signals," *Proceedings of the IEEE*, vol. 67, no. 6, pp. 930–949, 1979.
- [3] J. Middleton, L. und Sivaswamy, *Hexagonal Image Processing: A Practical Approach*, Springer, London, 2005.
- [4] F. Asharindavida, N. Hundewale, and S. Aljahdali, "Study on hexagonal grid in image processing," *IPCSIT*, vol. 45, pp. 282–288, 2012.
- [5] X. Hu, "Color filter patterns for image sensors," US Patent App. 10/307,860, 2004.
- [6] R. Ramanath, W. Snyder, and H. Qi, "Mosaic multispectral focal plane array cameras," in *SPIE Defense and Security Symposium, Orlando (Kissimmee)*, 2004, pp. 12–16.
- [7] K. Hirakawa and P. J. Wolfe, "New spatio-spectral sampling paradigm for imaging and a novel color filter array design," US Patent App. 12/516,908, 2010.
- [8] B. Gunturk, J. Glotzbach, Y. Altunbasak, R.W. Schafer, and R. M. Mersereau, "Demosaicking: Color filter array interpolation," *IEEE Signal Processing Magazine*, vol. 22, no. 1, pp. 44–54, 2005.
- [9] K. Hirakawa and T. Parks, "Adaptive homogeneitydirected demosaicking algorithm," *IEEE Transactions on Image Processing*, vol. 14, no. 3, pp. 360–369, 2005.
- [10] M. Schöberl, W. Schnurrer, A. Oberdörster, S. Fössel, and A. Kaup, "Dimensioning of optical birefringent anti-alias filters for digital cameras," in *2010 17th IEEE International Conference on Image Processing (ICIP)*. IEEE, 2010, pp. 4305–4308.